Journal of Power Sources 195 (2010) 7661–7668

Contents lists available at ScienceDirect

Journal of Power Sources

journal homepage: www.elsevier.com/locate/jpowsour

Conductive additive content balance in Li-ion battery cathodes: Commercial carbon blacks vs. *in situ* carbon from $LiFePO_4$/C composites

Verónica Palomares[a], Aintzane Goñi[a], Izaskun Gil de Muro[a], Iratxe de Meatza[b], Miguel Bengoechea[b], Igor Cantero[c], Teófilo Rojo[a,*]

[a] *Departamento de Química Inorgánica, Universidad del País Vasco UPV/EHU, P.O. Box. 644, 48080, Bilbao, Spain*
[b] *Energy Department, CIDETEC-IK4, P° Miramón 196, Parque Tecnológico de San Sebastián, 20009, San Sebastián, Spain*
[c] *Departamento I+D+i Nuevas Tecnologías, CEGASA, Artapadura, 11, 01013 Vitoria-Gasteiz, Spain*

ARTICLE INFO

Article history:
Received 26 March 2010
Received in revised form 7 May 2010
Accepted 25 May 2010
Available online 31 May 2010

Keywords:
Electrode composition
$LiFePO_4$/C composite
Carbon
Conductive additive

ABSTRACT

Two samples of commercial conducting carbon black and the carbon generated *in situ* during $LiFePO_4$/C composite synthesis from citric acid are studied, with the aim of finding out whether carbon from the composite can fulfil the same function as carbon black in the electrode blend for a Li-ion battery. For this purpose, the carbon samples are analyzed by several techniques, such as X-ray diffraction, Raman spectroscopy, transmission electron microscopy, granulometry, BET specific area and conductivity measurements. Different cathode compositions and component proportions are tested for pellet and cast electrodes. Electrochemical results show that a moderate reduction of commercial carbon black content in both kinds of cathodes, by adding more $LiFePO_4$/C composite, enhanced the electrochemical behaviour by around 10%. *In situ* generated carbon can partially replace commercial conducting carbon black because its high specific surface probably enhances electrolyte penetration into the cathode, but it is always necessary to maintain a minimum amount of carbon black that provides better conductivity in order to obtain a good electrochemical response.

1. Introduction

Since $LiFePO_4$ compound was first pointed out as a good candidate to be used as lithium-ion battery cathode [1], different strategies have proved to improve electrochemical behaviour of this olivine phase. Namely, aliovalent doping [2], coating with glassy phosphates [3] and producing $LiFePO_4$/C composites [4–11]. These composites can be produced by an intense grinding of the $LiFePO_4$ material with carbon, or by the addition of a carbon precursor during the synthesis (*in situ* generated carbon). This latter procedure has demonstrated to provide better electrochemical results [12]. *In situ* generated carbonaceous net performs two important functions. On the one hand, it provides a conducting web around the particles, making the electron conduction between them easier [13]. On the other hand, as carbon is present during the synthesis process, it is able to hinder particle growth and limits grain size [14].

$LiFePO_4$/C composites are blended with two other components in order to make the electrodes for electrochemical testing [15]. The first component is a conductive additive that usually consists on carbon black (also named furnace black). In the second place, PVDF (polyvinylidene fluoride) is commonly used as binder agent. Taking into account the existence of two carbon sources in the electrode, it is necessary to adjust the total carbon amount in the electrode to the minimum necessary, in order to maximize active material proportion and, thus, maximize electrode specific energy [16]. The question that arises from this approach is: can the carbon from the composite replace the conductive additive in the electrode mixture? In this sense, this work presents, on the one hand, a complete characterization of two kinds of commercial carbon blacks (*Timcal-Super P and Timcal-Super S*) and the carbon generated during the synthesis process of a $LiFePO_4$/C composite (*in situ* generated carbon). On the other hand, it searches for the best performing cathodic mixture, trying different proportions of active material/conductive additive, for cathodes prepared as pellets and by casting a slurry.

2. Experimental

2.1. Composite sample preparation

A $LiFePO_4$/C composite was prepared by freeze-drying method as it has been described before [17]. Starting solution contained stoichiometric amounts of citric acid hydrate monohydrate ($C_6H_8O_7{\cdot}H_2O$), ferrous acetate ($FeC_4H_6O_4$), lithium hydrox-

* Corresponding author. Tel.: +34 94 6012458; fax: +34 94 6013500.
E-mail address: teo.rojo@ehu.es (T. Rojo).

0378-7753/$ – see front matter © 2010 Elsevier B.V. All rights reserved.
doi:10.1016/j.jpowsour.2010.05.048

ide hydrate ($LiOH{\cdot}H_2O$) and ammonium dihydrogen phosphate ($NH_4{\cdot}H_2PO_4$). The obtained powders were calcined twice, at 350 and 600 °C, under nitrogen atmosphere, with an intermediate grinding in a planetary mill.

Characterization of the composite was made by powder diffraction, collected in a Philips PW1710 diffractometer working with Cu K-α radiation at room temperature. Elemental analysis by ICP-AES (PerkinElmer Optima 2000) of the sample agreed well with the stoichiometry of $LiFePO_4$. A PerkinElmer 2400CHN analyzer was employed for determining the carbon amount in the sample, and the result was 19 wt.%. Morphology of the composite was observed by transmission electron microscopy (TEM), using a Philips CM200 microscope.

Conductivity measurements of the synthesized composite were made on disc-shaped pellets at 25 °C with a frequency response analyzer connected to an Autolab PGSTAT30 potentiostat, over a frequency range from 1 MHz to 1 mHz with 100 mV amplitude.

2.2. Carbon sample preparation

A carbonaceous sample was also prepared, by annealing the carbon precursor used to prepare the composite – citric acid monohydrate – at the same temperatures that were used to synthesize the $LiFePO_4$/C material. This carbon sample was named *in situ* generated carbon.

2.3. Characterization of the furnace blacks and in situ generated carbon

Three carbon samples were characterized. In the first place, two commercial furnace blacks denominated Timcal-Super S and Timcal-Super P; and, in the second place, *in situ* generated carbon. Structural characterization of the three different samples comprised X-ray diffraction (XRD) and Raman spectroscopy, that was carried out at room temperature by using an InVia Renishaw RA100 spectrometer equipped with a Leica microscope DMLM. The 514 nm light from an Ar-ion laser was employed as excitation radiation. The spectra were recorded with the average of 10 scans and 20 mW power, and fitted with *Peakfit* software. Morphological characterization comprised transmission electron microscopy (TEM), made in a Philips CM200 microscope, and granulometry, that was carried out in a MalvernsizerS system. Volumetric conductivity was determined by four probe dc measurements using a Specac press, a Kethley 2400 intensity source and a Hewlett-Packard 34401A voltmeter. Brunauer–Emmet–Teller (BET) specific area of the carbonaceous materials was also determined by using a Micromeritics ASAP 2010 equipment.

2.4. Electrochemical measurements

The galvanostatic tests were conducted using Swagelok type cells assembled in an environmentally controlled dry box (dew point −80 °C). The negative electrode was a disk of lithium metal foil. A porous glass microfiber sheet soaked in a solution of 1 M $LiPF_6$ in EC:DMC (1:1 in volume) was placed between the two electrodes.

Two kinds of composite cathodes were made. The first ones were prepared by pressing the three electrode components ($LiFePO_4$/C composite, carbon black conductive additive and PVDF binder) to form thin pellets. Three different component percentages, named P1, P2 and P3, were used to prepare the pellet cathodes (Table 1). The second kind of cathodes was made by casting a viscous slurry on the current collector. This slurry was made of the three cathode components ($LiFePO_4$/C composite, conductive additive and PVDF binder) in n-dimethylformamide suspension. Table 2 shows the two different electrode components proportions that were tested, labelled E_80 and E_88. Four different blends of conductive additives (Timcal-Super P, Timcal-Super S, Timcal-Super P/KS6 Lonza graphite mixture and Timcal-Super S/KS6 Lonza graphite) were used in each electrode components proportion for casted electrodes (Table 3).

Table 1
Electrode compositions for P1, P2 and P3 pellet electrodes.

	$LiFePO_4$	*In situ* carbon	Conductive additive	Binder
P1	49%	12%	37%	2%
P2	66%	15%	17%	2%
P3	73%	17%	8%	2%

Table 2
Electrode proportions for casted cathodes.

	$LiFePO_4$	*In situ* carbon	Conductive additive	Binder
E_80	65%	15%	18%	2%
E_88	71%	17%	10%	2%

Table 3
Carbonaceous additives used for casted electrodes.

	E1	E2	E3	E4
Conductive additive/blend	Super P	Super S	Super P/KS6 Lonza	Super S/KS6 Lonza

Cyclic voltammetry (CV) measurements were carried out using a biologic multichannel potentiostat galvanostat (MPG) in the range from 1 to 4 V versus Li/Li^+ at 0.1 mV s^{-1}, whereas galvanostatic tests were made in an Arbin BT2000 Battery Tester at different C-rates, from C/40 to C/1. Ciclability tests were carried out by performing over 200 cycles at C/1 on the selected cathodes.

3. Results and discussion

3.1. Synthesis and characterization of the $LiFePO_4$/C composite and the carbon samples

The characterization of the composite sample showed the existence of a single crystalline phase: $LiFePO_4$. All the diffraction peaks from the powder X-ray diffractogram were indexed for the olivine structure [18] as it can be seen in Fig. 1. No peak corresponding to C was observed in this pattern.

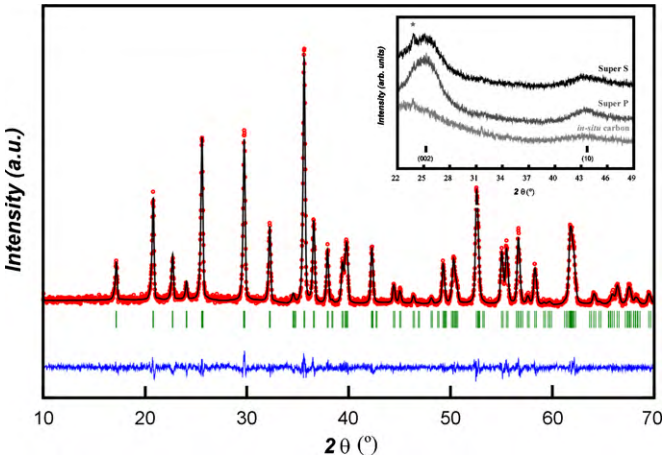

Fig. 1. X-ray diffractogram and fitted profile of $LiFePO_4$/C composite: experimental (circles), fitted (line) and difference between them (lower line). Inset: X-ray diffractogram of carbon samples. Diffraction maximum of the vaseline used as adhesive for the sample preparation is marked with a star.

Table 4
Characteristic parameters of the samples obtained from the fitting of the Raman spectra.

	Timcal-Super P	Timcal-Super S	*In situ* carbon
D/G	1.24	0.93	1.61
sp^3/sp^2	2.44	2.48	3.96

X-ray diffractograms of the three carbon samples (Super P, Super S and *in situ* C) are compiled in the inset of Fig. 1, showing in all cases a broad band around 25°. This band corresponds to graphite <0 0 2> reflection, and it indicates the presence of graphene layers in the materials. The presence of a broad band, instead of a narrow diffraction peak at 25°, is associated with the common structural disorder in this kind of carbon blacks [19,20]. As it can be observed, *in situ* formed carbon presents a broader band than furnace black samples, whereas Super P shows the narrowest one among the three carbon samples. So, *in situ* produced carbon has greater amorphous character than furnace blacks, which is coherent with a low temperature synthesized carbon. As Super P sample shows the narrowest band, it can be deduced that this material presents a more ordered structure than Super S carbon.

Raman spectra of the three samples are depicted in Fig. 2. As it can be seen, typical D and G bands of carbon appear around 1340 and 1580 cm^{-1}, respectively, for all the three materials. However, the relative intensities of the D and G bands as well as their shape change between samples. When analyzing carbonaceous materials, G band (1580 cm^{-1}) is assigned to the E_{2g} graphite mode, and D band (1340 cm^{-1}) is associated to A_{1g} mode, that is related to the breakage of symmetry occurring at the edges of graphite sheets. The relative intensity of the D band *vs.* G band is attributed to increased carbon disorder, for example, in microcrystalline graphite [21]. Thus, the similar D and G band intensity in the Raman spectra of these samples is consistent with highly disordered carbon.

In order to resolve the Raman spectra, a standard peak deconvolution procedure was applied. Band fitting with two carbon D and G lines did not give accurate results, thus four Gaussian bands were necessary to account for the observed Raman features with minimum error. Those four band locations were around 1200, 1347, 1510, and 1585 cm^{-1} in all spectra, but the positions and intensities of these bands varied a little between samples. The bands at 1585 and 1347 cm^{-1} correspond to G and D bands, as it has been explained before. The bands at 1194 and 1510 cm^{-1}, which are often observed in highly amorphous carbonaceous materials, were assigned to tetrahedral and sp^3-type carbon [22]. An additional band at 1620 cm^{-1} had to be added to Timcal-Super P spectrum fitting. This band is also related to disordered carbons (see Ref. [21]).

Characteristic parameters of the samples obtained from the fitting of the Raman spectra are D/G and sp^3/sp^2 ratio (Table 4). This latter is obtained by dividing the area of sp^3 carbon bands (1194, 1347, 1510 and 1620 cm^{-1}) and sp^2 G band (1585 cm^{-1}). Both commercial carbon samples present very similar sp^3/sp^2 ratios, being the quantity of sp^3 hybridized carbon 2.5 times the amount of sp^2-type carbon. *In situ* generated carbon has the greatest D/G and sp^3/sp^2 ratios. These ratios indicate that *in situ* produced carbon contains fewer and shorter graphene layers (sp^2 carbon) than commercial samples and so, it presents the lowest degree of graphitization.

Morphology of the composite and the three carbon samples was determined by TEM. As it can be appreciated in Fig. 3a, $LiFePO_4$/C sample consists of aggregates of approximately 100 nm size. These aggregates are made up of both $LiFePO_4$ particles and C, as it has been seen in other samples prepared by freeze-drying process (see Ref. [14]). The exact primary phosphate particle size cannot be seen because it was not possible to break up the aggregates to observe particle limits clearly, but it is below 100 nm.

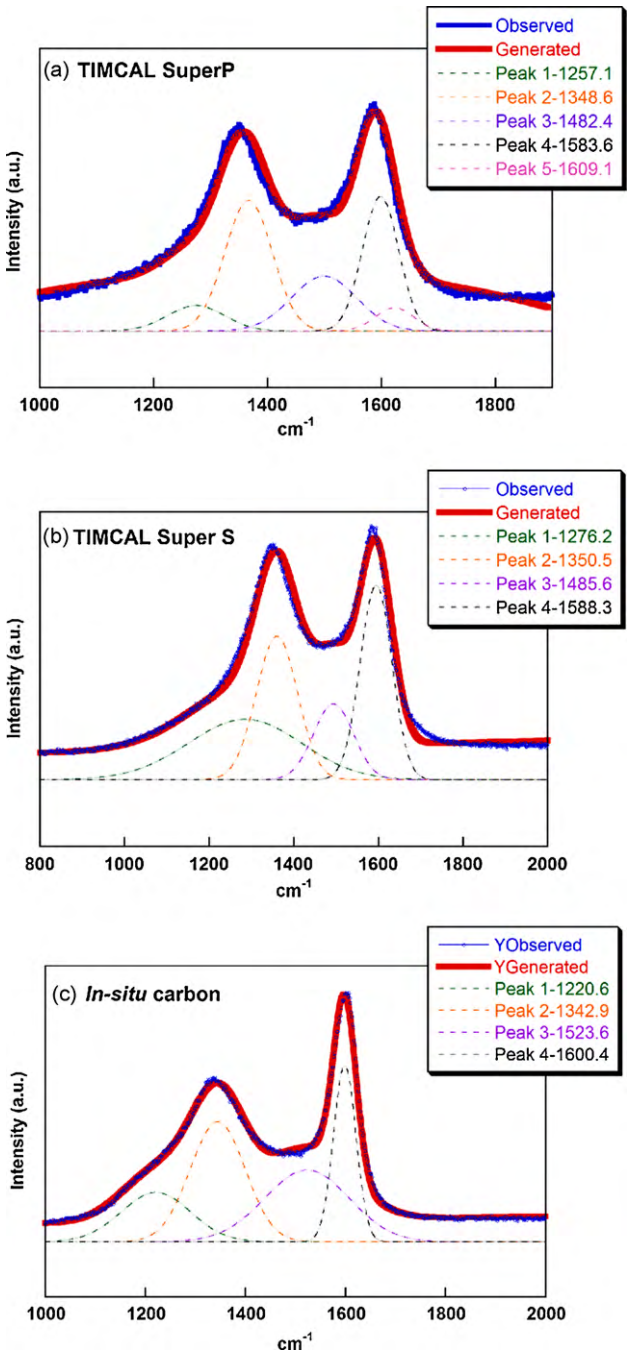

Fig. 2. Raman spectra and fitting of the three carbon samples.

Fig. 3b and c depicts micrographies of both Super P and Super S carbon samples, that exhibit typical morphology of furnace blacks. The structure of these carbon blacks is determined by their synthesis process. Furnace blacks are produced by partial combustion or by thermal decomposition of liquid or gaseous hydrocarbons. This combustion or decomposition causes the formation of extremely small carbon nodules that come from hydrocarbon combination, form the aromatic layers and condense to create spherical particles. These little nodules grow and become groups by coalescence, forming branched structures or aggregates. Aggregates are strongly attracted by electrostatic forces, and form bigger structures – agglomerates – in the last step of the synthesis process. In this way, Super P and Super S samples micrographs show two features of carbon blacks: small spherical carbon particles – nodules – that

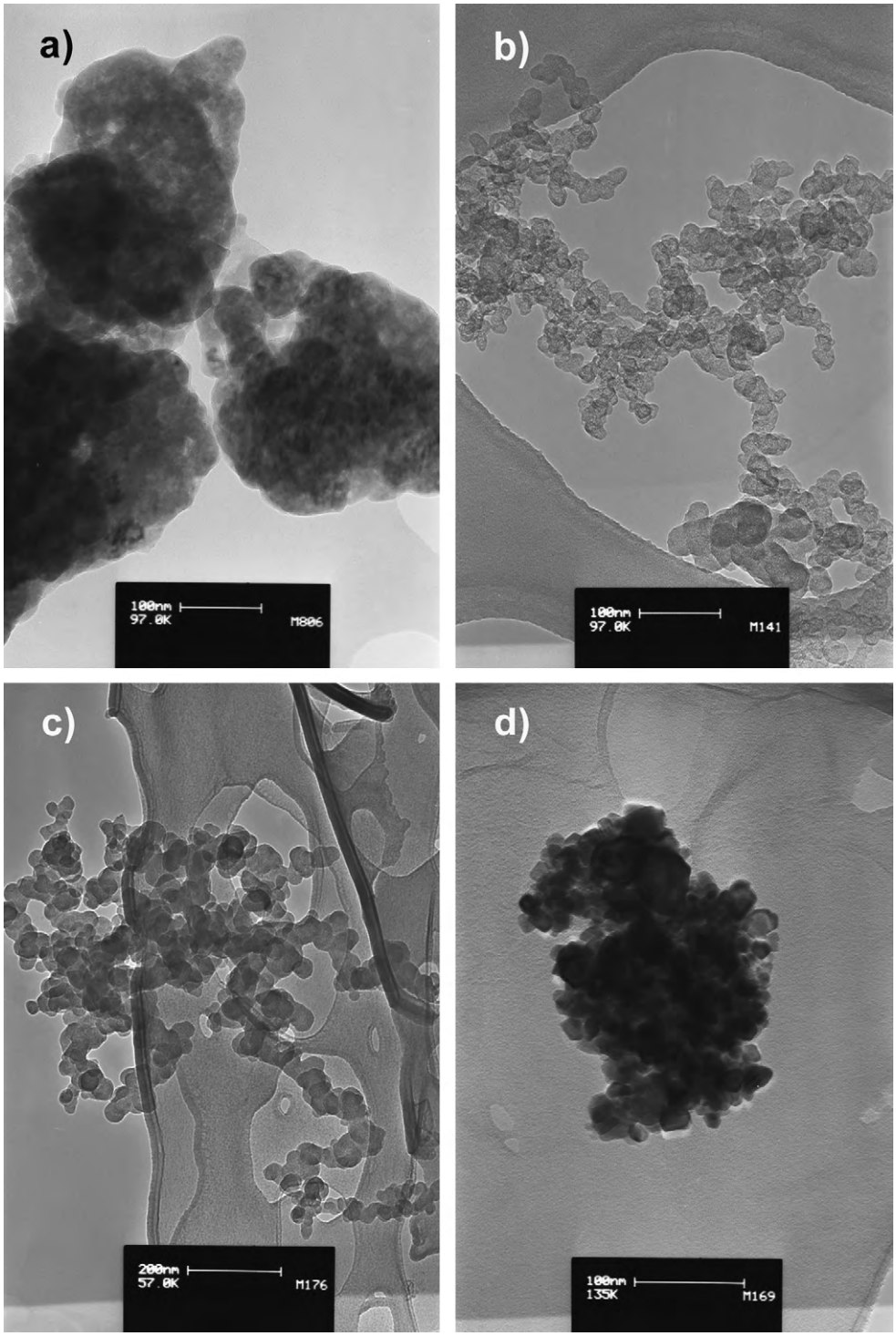

Fig. 3. TEM micrographs of (a) $LiFePO_4$/C composite; (b) Timcal-Super P; (c) Timcal-Super S; (d) and (e) *in situ* produced carbon.

form branched structures – aggregates – by coalescence. Nodules have about 20–50 nm diameter, and aggregates are bigger than 100 nm. The big agglomerates are not observed by this technique because they are destroyed by the dispersion of aggregates during the sample preparation. On the other hand, carbon generated during $LiFePO_4$/C synthesis process (Fig. 3d and e) is slightly different. Fig. 3d exhibits a more compact morphology, with non-branched aggregates between 100 and 300 nm size, but 20 nm isolated nodules are also observed in Fig. 3e. The three carbon samples present the same nodule size, in spite of their different origin. Differences in nodule aggregation modes between furnace blacks and *in situ* made carbon come from the distinct synthesis process for both carbon types. In the case of *in situ* generated carbon, more compact aggregates appear because this carbon comes from the pyrolysis of solid grains of citric acid, whereas the thermal decomposition of liquid or gaseous hydrocarbons favours the formation of lighter structures, of branched aggregates. Thus, *in situ* generated carbon shows a different aggregation mode from commercial carbon blacks.

Once nodules and aggregate sizes were known for the three carbons, granulometry was used in order to know the size of the

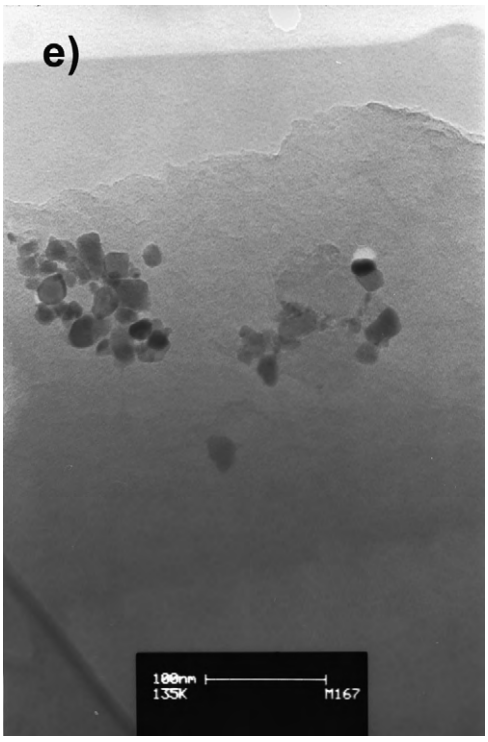

Fig. 3. (*Continued*)

agglomerates, the biggest structures in carbonaceous samples, in the scale of micrometers. In this sense, it can be seen that the carbonaceous materials show different distribution modes (Fig. 4). In the first place, Super P exhibited a three-modal distribution, showing a narrow peak at 51.5 μm that is the most populated one – from 10 to 100 μm. In the second place, Super S presents a unique distribution centred at 33 μm, broader than in the previous case – from 5 to 100 μm. In the third place, *in situ* produced carbon also exhibited a unique but very broad distribution around 45.4 μm – from 1 μm to more than 100 μm. This is consistent with the structures observed in TEM micrographs, where the existence of isolated nodules and compact aggregates in *in situ* carbon can cause greater dispersion in particle sizes.

Conductivity of all materials (Super P, Super S, *in situ* carbon and $LiFePO_4$/C composite) was obtained. Volumetric conductivity measurements were made on the three carbon samples. It was not possible to reach quasi-graphitic behaviour pressure, but, as it can be observed in Fig. 5, there exists a three orders of magnitude difference between commercial samples and *in situ* generated carbon. The carbon blacks exhibit a conductivity in the range of 5–30 $S\,cm^{-1}$, whereas *in situ* generated carbon presents values about $3 \times 10^{-4}\,S\,cm^{-1}$ at the same pressures. This low conductivity is consistent with its lower content on sp^2 carbon detected in Raman spectra fitting, which is responsible for electronic conduction.

The conductivity of the $LiFePO_4$/C composite was measured by impedance spectroscopy. A value of $8.0 \times 10^{-7}\,S\,cm^{-1}$ was obtained, which is two orders of magnitude greater than the theoretical value of pristine $LiFePO_4$ ($10^{-9}\,S\,cm^{-1}$) (see Ref. [1]). This increase in the conductivity is due to the presence of carbon in the sample, 19% weight, but it is slight because of the low conductivity of the *in situ* generated C.

Carbon materials characterization was completed by BET surface analysis. The obtained specific area values were 60.62, 43.76 and 71.46 $m^2\,g^{-1}$, for Super P, Super S and *in situ* produced carbon respectively. Thus, carbon generated in our laboratory showed the greatest specific area of the three samples, followed by Super P and Super S. This fact agrees with other features observed during samples characterization, such as the great dispersion of *in situ* carbon agglomerate size shown in granulometry and the presence of isolated nodules in it. Specific surface area is an important parameter for good electrode function, because a high specific area favours electrolyte penetration in the cathode, and, thus, enhances lithium ions access to active material.

All parameters obtained during commercial carbon samples characterization agreed well with those supplied by the manufacturers (TIMCAL).

Taking into account the complete characterization made over the three carbon materials (Table 5), it can be deduced that there exist several differences between commercial furnace blacks and carbon generated in $LiFePO_4$/C composites. *In situ* generated carbon, in spite of its great superficial area, presents high structural disorder, which is not favourable to a good electrochemical performance [23], and does not have enough conductivity to fulfil the function of conductive additive in these cathodes. Thus, it can be said that there must always be a portion of carbon black in the cathodic mixture to get a good electrochemical behaviour.

3.2. Electrochemistry. Study on electrode composition

After the study of the three different kinds of carbon, several pellet-cathodes were prepared, increasing $LiFePO_4$/C composite proportion from 61 to 90 wt.% and, thus, decreasing the usual 30% furnace black content down to 8% (Fig. 6). It must be noted that, for these electrodes, binder proportion was adjusted to 2 wt.% in order to increase composite proportion up to 90 wt.% while preserving a small amount of carbon conductive additive in the mixture. Fig. 7 depicts relative specific capacities for the different electrodic blends at diverse C-rates, from C/40 to C/1. P1 electrode, the one used until the moment in our laboratory is taken as reference. Table 6 shows the different specific capacities obtained for P1 blend at the different C-rates. As it can be seen in Fig. 7, the elec-

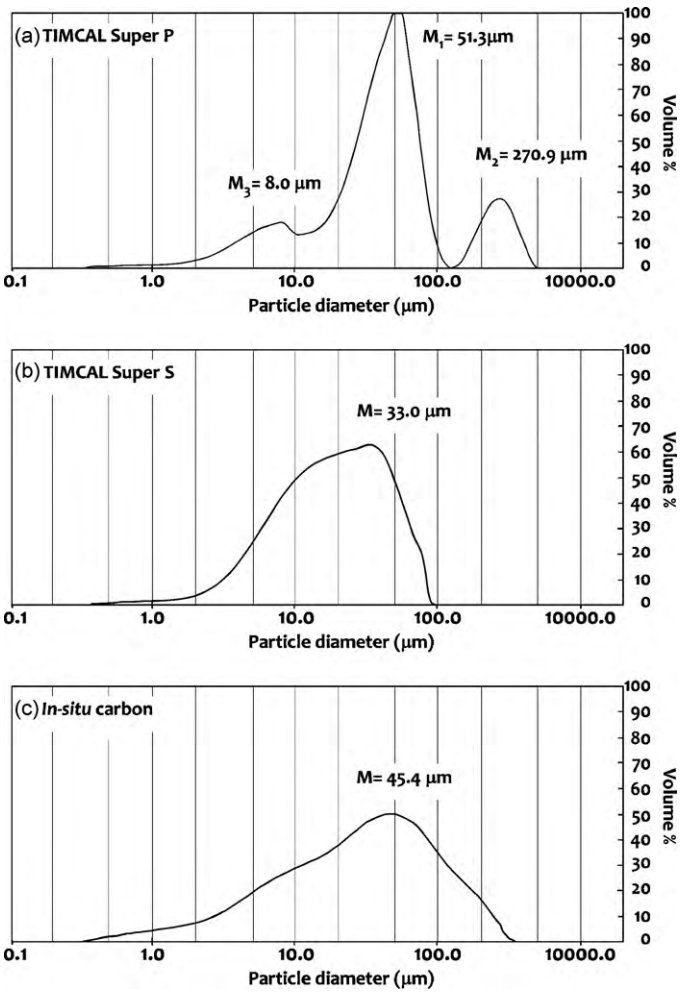

Fig. 4. Granulometry curves for (a) Timcal-Super P; (b) Timcal-Super S; (c) *in situ* produced carbon. Statistical modes (M) are indicated for each material.

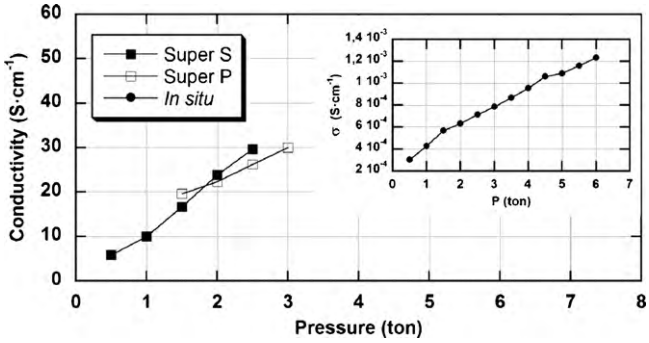

Fig. 5. Conductivity vs. pressure plot for the carbon samples. *In situ* carbon volumetric conductivity is depicted in the inset.

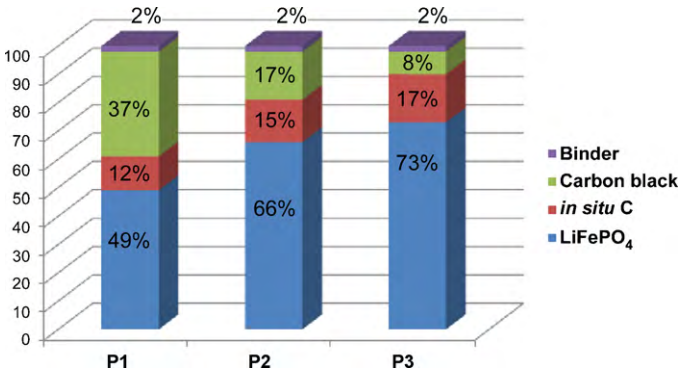

Fig. 6. Composition of pellet electrodes P1, P2 and P3.

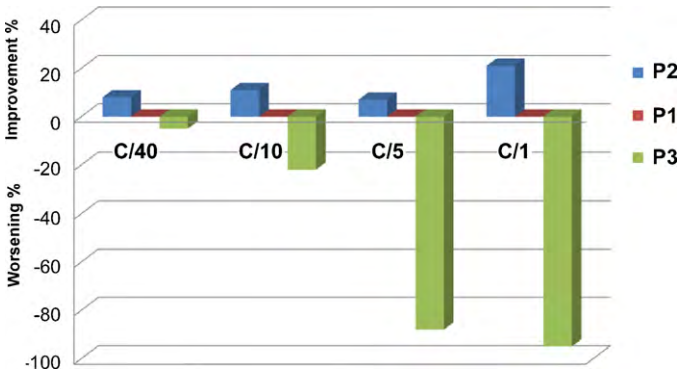

Fig. 7. Relative specific capacities (%) of P2 and P3 with respect to P1.

Table 6
Specific capacities obtained for P1 electrode.

	C/40	C/10	C/5	C/1
P1	155 mAh g^{-1}	140 mAh g^{-1}	128 mAh g^{-1}	120 mAh g^{-1}

trode P2 made with an 81 wt.% composite (66% $LiFePO_4$) showed an improvement, at every charge/discharge rates, from the specific capacity (measured in mAh per gram of $LiFePO_4$) offered by P1, with 61 wt.% composite (49% $LiFePO_4$). On the other hand, electrode with greater proportion of active composite, P3, does not represent any improvement with respect to P1. It is interesting to note that the specific capacity provided by the P3 sample shows comparatively poorer results as charge/discharge rate is increasing from 40 to 1 h. This fact evidences the importance of a good conductivity in the cathode for a rapid electrochemical response of the electrode.

Fig. 8 depicts the *plateaus* from charge-discharge curves for P1, P2 and P3 at C/40 and C/10. Polarization of the electrodes is shown in the plot. As it can be seen, P1 and P2 posses very close polarization values at C/40, of about 0.041 V, whereas this parameter is equal for both blends at C/10, with a value of 0.054 V. This way, at moderate rates P2 offers greater specific capacity values and a

Table 5
Summary of carbon samples characterization.

		Super P	Super S	*In situ* carbon
Raman spectroscopy	D/G	1.24	0.93	1.61
	sp^3/sp^2	2.44	2.48	3.96
Transmission electron microscopy	Nodules	17–50 nm	17–50 nm	17–21 nm
	Aggregates	>100 nm	>100 nm	Compact ~100 nm and isolated nodules
Granulometry	Agglomerates	51 µm (narrow)	33 µm (broad)	45 µm (very broad)
Volumetric conductivity		5–30 S cm^{-1}	5–30 S cm^{-1}	3×10^{-4} S cm^{-1}
Specific surface		60.63 m^2 g^{-1}	43.76 m^2 g^{-1}	71.46 m^2 g^{-1}

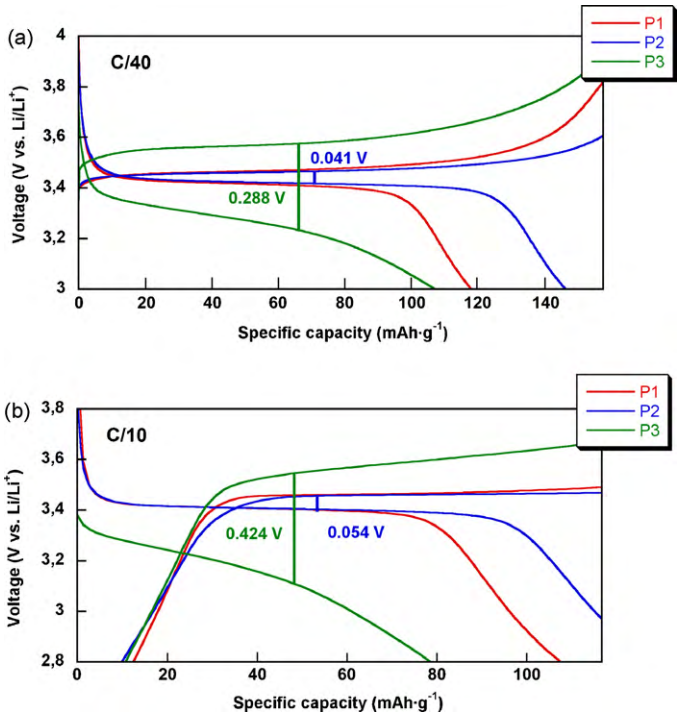

Fig. 8. Polarization of charge–discharge curves for P1, P2 and P3 at (a) C/40 and (b) C/10.

polarization value similar to P1. Thus, it can be concluded that P2 is a better electrodic blend. On the other hand, P3, due to its low conductive carbon content, presents greater polarization values (7 times higher) even at low rates, 0.288 V at C/40 and 0.424 V at C/10.

With regard to pellet electrodes, it can be said that a 30% of carbon in the electrodic mixture seems to be an adequate proportion, maintaining a suitable amount of conductive furnace black around 15%. The results indicate the tolerance of the system to greater active material proportions than commonly used before, but set a limit in this increase on composite proportion by the need of an adequate conductivity.

Casted electrodes were prepared using different kinds of conductive additive. This type of electrodes, prepared by casting a fine layer of slurry on the current collector, are thinner and more similar to the commercial ones. The different kinds of conductive additive employed were the two furnace blacks that have been characterized before (Timcal-Super P and Super S), and their mixtures with a commercial graphite (KS6 Lonza). These carbon black/graphite blends were tested on the basis of previous studies on $LiCoO_2$ cathodes, which pointed out that the presence of graphite as part of the conductive additive provided better utilization of the active material and longer electrode life [24]. In this case, two different proportions were tested on the 4 types of blends, using 80 or 88% composite to make the electrode, as it is shown in Fig. 9. The electrodes were cycled at C/5 and at C/1. Fig. 10 depicts relative specific capacities for the electrodes taking as reference the standard composition, corresponding to an 80% composite, 18% Super S carbon and 2% binder (PVDF). The specific capacities obtained for this electrode blend, denominated E2_80, are 107 and 88 mAh g^{-1} at C/5 and C/1 respectively.

The relative specific capacities depicted in Fig. 10 demonstrate that the addition of KS6 Lonza graphite does not improve electrochemical behaviour of the cathodes with respect to using just carbon blacks, in spite of the higher conductivity of graphite. This can be due to an ineffective intimate mixing of the cathodic blend, caused by the great difference in the grain sizes of the KS6 Lonza

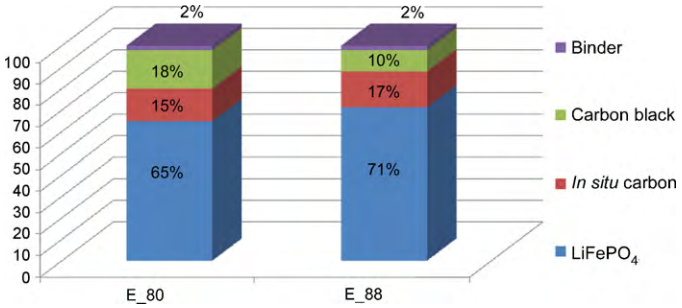

Fig. 9. Composition of casting electrodes E_80 and E_88.

graphite (6 μm flat particles (see Ref. [24]) and the rest of the cathodic components (particles <100 nm).

Effectiveness of the different furnace blacks and influence of the two compositions tested can be also analyzed from data in Fig. 10. First of all, it must be noted that the use of Super P carbon (E1 electrodes) provokes in all cases an improvement on the electrode specific capacity, for example, of 11 and 7% for E1_80 electrode at C/5 and C/1, respectively. Secondly, E_88 electrodes showed better specific capacities than the standard one, using either Super S or Super P furnace black as additive. Thus, two conclusions can be achieved from these data. On the one hand, Super P furnace black provides the best results as conductive additive in cathodes for Li-ion batteries based on $LiFePO_4$/C composites produced by freeze-drying process, which is consistent with the results obtained during carbon sample characterization. As we have pointed out previously, Super P carbon possesses adequate order degree, high specific surface and good conductivity. These features make Super P furnace black the best conductive additive among the three carbon blacks analyzed.

On the other hand, an improvement on the electrochemical behaviour at every rates has been observed when using a higher $LiFePO_4$/C composite proportion than usual, reducing the carbon black amount to 10% Super P.

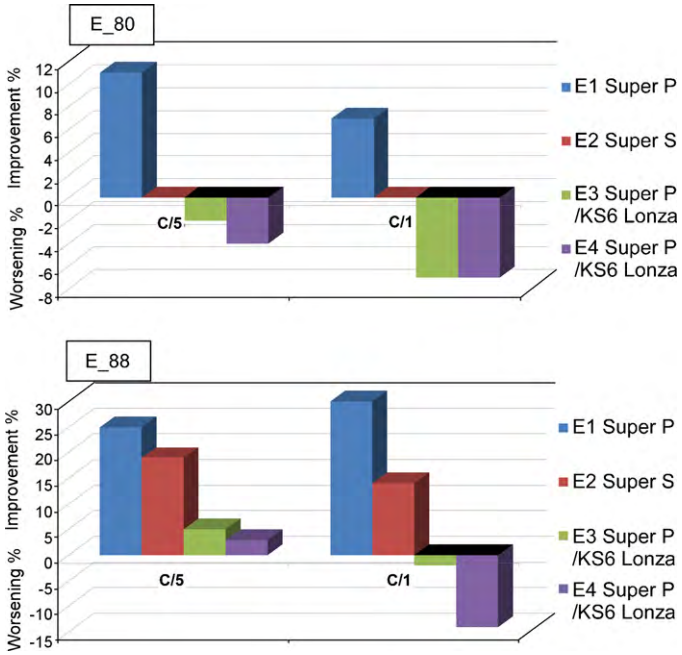

Fig. 10. Relative specific capacities for casting electrodes taking as reference the standard composition used in our laboratory, that corresponds to an 80% composite, 18% Super S carbon and 2% binder (PVDF).

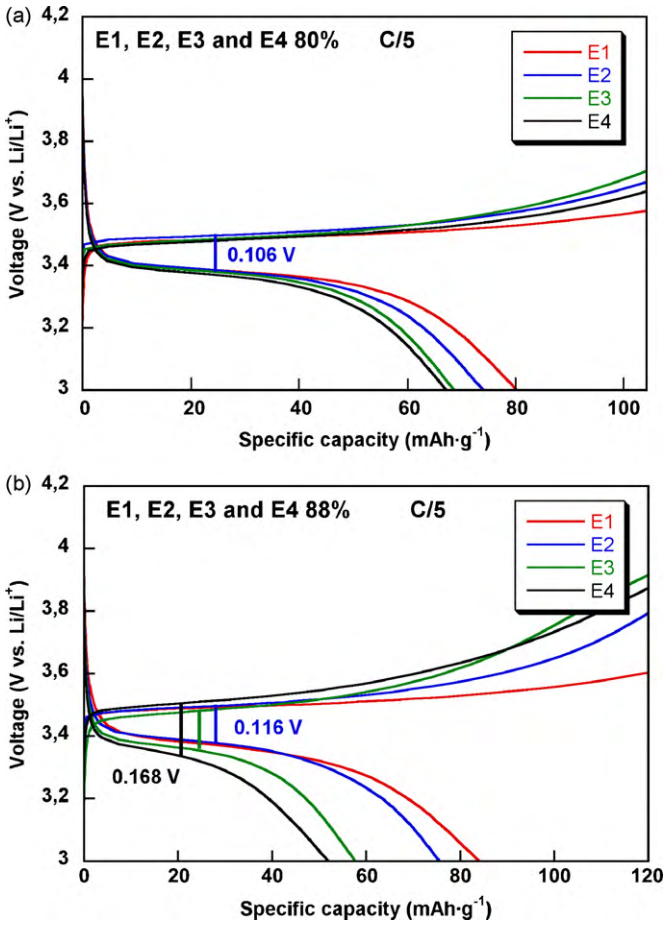

Fig. 11. Polarization of charge–discharge curves for E_80 and E_88 casting electrodes at C/5.

Fig. 11 shows polarization values of charge–discharge curves for E_80 and E_88 electrodes at C/5. No great difference between diverse compositions is detected for E_80 and E_88 electrodes. Only E_88_4 electrode presents different polarization value, being greater than the others. The absence of an evolution in polarization values can be partially responsible for the bad results obtained using carbon black/graphite blends in the electrodes. This way, graphite present in the electrodic blend is not able to enhance cathode conductivity more than commercial carbon blacks, thus the use of graphite in the electrodic blend does not represent any improvement in electrochemical behaviour of the material.

It must be noted that, whereas in casted electrodes an 88% composite provided the best electrochemical performance, 90% composite proportion did not give good results in pellet electrodes. This is due to the greater thickness of pellet cathodes. This fact implies a greater need of conductive additive in pellet electrode composition in order to provide good access of Li^+ ions and electrons to active material.

Thus, as it can be deduced from the electrochemical tests, *in situ* generated carbon can replace partially the conductive additive in cathodes for lithium-ion batteries, because its great specific area and its intimate contact with the active $LiFePO_4$ material favours the electrochemical performance. But, the structural disorder hinders a high conductivity and it does not allow a complete substitution of the conductive additive in electrode blend. This way, it is possible to reduce conductive additive proportion in $LiFePO_4$/C-based cathodes from the usual quantity but not completely eliminated from the electrode.

4. Conclusions

This work presents a complete characterization of commercial furnace blacks, such as Timcal-Super P and Timcal-Super S; together with a carbon sample from a $LiFePO_4$/C composite. Structural, morphological and electrochemical characterization of the three materials indicated that there exist several differences between furnace blacks and *in situ* generated carbon. In spite of its high specific surface, *in situ* produced carbon presents high disorder, which is not favourable to a good electrochemical performance, and does not have enough conductivity to act as conductive additive in these cathodes.

Electrochemical tests made on both casting and pellet electrodes showed that a moderate increase on composite content enhanced electrochemical behaviour, but a great increase on it caused low specific capacity. This fact confirms what it was observed during carbon materials characterization. *In situ* generated carbon can replace partially commercial conductive carbon black because its high specific surface enhances electrolyte penetration into the cathode, but it is always necessary a minimum amount of furnace black that provides conductivity in order to get a good electrochemical behaviour.

Acknowledgements

This work was financially supported by the Ministerio de Educación y Ciencia (PTR95.0939.01, MAT2007-66737-C02-01; MAT2007-64486-C07-05), the Universidad del País Vasco/Euskal Herriko Unibertsitatea (GIU06-11) and CEGASA GROUP, which we gratefully acknowledge. V.P. thanks UPV/EHU for a grant. We would like also to thank Amane Lago for her kind assistance with the electrochemical measurements.

References

[1] A.K.M. Padhi, K.S. Nanjundaswamy, J.B. Goodenough, J. Electrochem. Soc. 144 (1997) 1188–1194.
[2] S.Y. Chung, J.T. Bloking, Y.M. Chiang, Nat. Mater. 1 (2) (2002) 123–128.
[3] B. Kang, G. Ceder, Nature 458 (2009) 190–193.
[4] S.J. Kwon, C.W. Kima, W.T. Jeong, K.S. Lee, J. Power Sources 137 (2004) 93–99.
[5] E.M. Bauer, C. Bellitto, G. Righini, M. Pasquali, A. Dell'Era, P.P. Prosini, J. Power Sources 146 (2005) 544–549.
[6] S.T. Yang, N.H. Zhao, H.Y. Donga, J.X. Yang, H.Y. Yue, Electrochim. Acta 51 (2005) 166–171.
[7] S. Luo, Z. Tang, L. Junbiao, Z. Zhang, Ceram. Int. 34 (2008) 1349–1351.
[8] J. Liu, J. Wang, X. Yan, X. Zhang, G. Yang, A.F. Jalbout, R. Wang, Electrochim. Acta 54 (2009) 5656–5659.
[9] Z.R. Chang, H.J. Lva, H.W. Tang, H.J. Li, X.Z. Yuan, H. Wang, Electrochim. Acta 54 (2009) 4595–4599.
[10] Z. Zaghib, A. Mauger, J.B. Goodenough, F. Gendron, S.S. Zhang (Eds.), Advanced Materials and Methods for Lithium-ion Batteries, Research Signpost, Trivandrum, 2007.
[11] Y. Wang, Y. Wang, E. Hosono, K. Wang, H. Zhou, Angew. Chem. 47 (2008) 7461–7465.
[12] J.K. Kim, G. Cheruvally, J.H. Ahn, G.C. Hwang, J.B. Choi, J. Phys. Chem. Solids 69 (2008) 2371–2377.
[13] H.C. Shin, W.I. Cho, H. Jang, Electrochim. Acta 52 (2006) 1472–1476.
[14] V. Palomares, A. Goñi, I. Gil de Muro, I. de Meatza, M. Bengoechea, I. Cantero, T. Rojo, J. Electrochem. Soc. 156 (2009) A817–A821.
[15] G. Liu, H. Zheng, A.S. Simens, A.M. Minor, X. Song, V.S. Battaglia, J. Electrochem. Soc. 154 (2007) A1129–A1134.
[16] Z. Chen, J.R. Dahn, J. Electrochem. Soc. 149 (2002) A1184–A1189.
[17] V. Palomares, A. Goñi, I. Gil de Muro, I. de Meatza, M. Bengoechea, O. Miguel, T. Rojo, J. Power Sources 171 (2007) 879–885.
[18] D. Destenay, Mem. Soc. Roy. Sci. Liege 10 (1950) 5–28.
[19] A. Sharma, T. Kyotani, A. Tomita, Carbon 38 (2000) 1977–1984.
[20] B.E. Warren, J. Chem. Phys. 2 (1934) 551–555.
[21] R. Vidano, D.B. Fischbach, J. Am. Ceram. Soc. 61 (1–2) (1978) 13–17.
[22] F. Tuinstra, J.L. Koenig, J. Chem. Phys. 53 (1970) 1126–1130.
[23] M.M. Doeff, Y. Hu, F. McLarnon, R. Kostecki, Electrochem. Solid State Lett. 6 (2003) A207–A209.
[24] J.K. Hong, J.H. Lee, S.M. Oh, J. Power Sources 111 (2002) 90–96.